

Mantle kinematics and formation of commarginal shell sculpture in Bivalvia

TAKAO UBUKATA

Department of Earth Sciences, Shizuoka University, Otani 836, Shizuoka, 422 Japan

Received 4 December 1996 ; Revised manuscript accepted 1 April 1997

Abstract. The geometry of the commarginal shell sculpture and internal microgrowth pattern in 82 species of the Bivalvia were analyzed both theoretically and empirically. Two major categories were recognized in the geometry of internal microgrowth increments; 1) the regular type, which consists of regularly arranged curves, being mutually parallel in the sections and maintaining their morphology during growth independent of the sculpture pattern, and 2) the undulated type, with undulated microgrowth increments along the folds of prominent sculpture. For the former category, geometric patterns of the sculpture and increments of actual specimens were well reproduced by computer simulations under the condition that the sculpture is originated by mantle extension and shrinkage. In the latter case, mantle bulging or bending appears to produce a plicated shell folding, although sculpture formation cannot be simulated by the model adopted in this study.

Key words: Bivalves, microgrowth increments, shell sculpture, theoretical morphology

Introduction

The external shell sculpture of molluscs and brachiopods have been taken for granted not only as taxonomically useful, but also as functionally significant characters (Wrigley, 1948; Rudwick, 1968; Stanley, 1969, 1970; Seilacher, 1972, 1974; Savazzi *et al.*, 1982; Signor, 1982; Savazzi, 1986). On the other hand, two-dimensional patterns of ornamentation on the external shell surface have attracted much attention from theoretical morphologists (Waddington and Cowe, 1969; Lindsay, 1982a, 1982b; Hayami and Okamoto, 1986; Meinhardt, 1984; Meinhardt and Klingler, 1987; Gunji, 1990; Ackerly, 1992). However, only a few authors have focused on the role of the mantle (Carter, 1967; Checa, 1994). Analyzing the mantle kinematics during shell growth is necessary for understanding the mantle-shell relationship in which the mantle forms the shell and the shell constrains the shape of the mantle (Savazzi, 1990; Seilacher and Gunji, 1993). For such an analysis, the commarginal sculpture in bivalves is particularly suitable because it is geometrically simple and is widespread in many taxa.

Commarginal shell sculpture in bivalves consists of a series of conformable curves with a concentric direction on the outer shell surface determined by the former position of the shell. Cox (1969) suggested that the commarginal sculpturing resulted from a rhythmic change in the rate of secretion of shelly matter, while Seilacher (1985) assumed periodic bulging of the mantle edge for its origin. However, no attempts have yet been made to estimate parameters determining the sculptural patterns in general.

The present work analyzes the geometric pattern of radially sectioned bivalve shell and attempts to model the formation of the commarginal shell sculpture from the viewpoint of mantle kinematics. The relationship between internal microgrowth increments and the sculptural pattern is especially taken into consideration. The sequences of internal microgrowth increments have been regarded as the record of periodic time series in many cases (Pannela and MacClintock, 1968; Jones *et al.*, 1978; Jones, 1985; Tanabe, 1988; Tanabe and Oba, 1988). Then the internal microgrowth increments are also the record of the mantle kinematics because the mantle is in contact with the inner surface of the shell during shell secretion.

Material and method

In order to clarify the microscopic features of the shell, microscopic observations in radial and vertical sections were made for all species examined. A total of 82 extant and fossil bivalve species listed in Table 1 were studied. Each species is represented by one or a few specimens. Most specimens were collected at various localities around the Japanese Islands and the Philippines by myself, but some specimens were selected from the collection of the University Museum, University of Tokyo. All the figured specimens are preserved in the University Museum, University of Tokyo (UMUT).

A single valve for each specimen was first cut using an electric saw vertical to the outer shell surface along the radial direction. Pieces of the sections were embedded in

Table 1. List of materials examined.

Family	species	locality	
Arcidae	<i>Arca navicularis</i>	Shikanoshima, Fukuoka, western Japan	
	<i>A. boucardi</i>	Morozaki, Aichi, Central Japan	
	<i>Barbatia amygdarumtortum</i>	Iriomote Is., Okinawa, southwest Japan	
Glycymerididae	<i>Anadara antiquata</i>	Honda Bay, Palawan, southwest Philippines	
	<i>Glycymeris yessoensis</i>	Sarufutsu, Hokkaido, northern Japan	
Mytilidae	<i>Mytilus grayanus</i>	Samani, Hokkaido, northern Japan	
	<i>M. galloprovincialis</i>	Yokohama, Kanagawa, Central Japan	
	<i>M. californianus</i>	Neah Bay, Washington, USA	
	<i>Septifer bilocularis</i>	Turtlecove Is., Palau	
	<i>Modiolus modiolus</i>	Samani, Hokkaido, northern Japan	
Inoceramidae	<i>Inoceramus lobetsensis</i>	Obira, Hokkaido, northern Japan	
	<i>I. uwajimensis</i>	Obira, Hokkaido, northern Japan	
Pteriidae	<i>Pinctada margaritifera</i>	Ishigaki Is., Okinawa, southwest Japan	
	<i>P. fucata</i>	Misaki, Kanagawa, Central Japan	
Isognomonidae	<i>Isognomon perna</i>	Iriomote Is., Okinawa, southwest Japan	
	<i>I. isognomonum</i>	San Luice, Bathangas, Philippines	
	<i>I. legumen</i>	Iriomote Is., Okinawa, southwest Japan	
Malleidae	<i>Malleus regula</i>	Iriomote Is., Okinawa, southwest Japan	
Pinnidae	<i>Pinna muricata</i>	Honda Bay, Palawan, southwest Philippines	
	<i>Atrina kinoslutai</i>	Amakusa, Kumamoto, western Japan	
Limidae	<i>Lima vulgaris</i>	Turtlecove Is., Palau	
Ostreidae	<i>Crassostrea lineata</i>	Iriomote Is., Okinawa, southwest Japan	
	<i>Crassostrea gigas</i>	Misaki, Kanagawa, Central Japan	
Plicatulidae	<i>Plicatula muricata</i>	Misaki, Kanagawa, Central Japan	
Pectinidae	<i>Cryptopecten vesiculosus</i>	Misaki, Kanagawa, Central Japan	
	<i>Chlamys swifti</i>	Wakkanai, Hokkaido, northern Japan	
	<i>Patinopecten yessoensis</i>	Wakkanai, Hokkaido, northern Japan	
	<i>Spondylus squamosus</i>	Iriomote Is., Okinawa, southwest Japan	
	<i>S. barbatus</i>	Sagami Bay, Kanagawa, Central Japan	
Unionidae	<i>Inversidens reiniana</i>	Lake Biwa, Shiga, Central Japan	
	<i>Unio biwae</i>	Lake Biwa, Shiga, Central Japan	
	<i>Lanceolaria grayana oxyrhyncha</i>	Lake Biwa, Shiga, Central Japan	
	<i>Cristaria plicata</i>	Lake Biwa, Shiga, Central Japan	
	<i>Lamprotula rochechoarti</i>	Lake Tung-ting, China	
	<i>Lamprotula</i> sp.	Lake Tung-ting, China	
Trigoniidae	<i>Neotrigonia margaritacea</i>	French Is., Australia	
Lucinidae	<i>Codakia tigerina</i>	Panglao Is., Cebu, southern Philippines	
	<i>Cardita leana</i>	Misaki, Kanagawa, Central Japan	
Carditidae	<i>Begonia seniorbiculata</i>	Honda Bay, Palawan, southwest Philippines	
	<i>Megacardita ferruginosa</i>	Misaki, Kanagawa, Central Japan	
Chamidae	<i>Chama brassica</i>	Honda Bay, Palawan, southwest Philippines	
Astartidae	<i>Tridonta alaskensis</i>	Etorofu Is., Hokkaido, northern Japan	
Cardiidae	<i>Fragum unedo</i>	Iriomote Is., Okinawa, southwest Japan	
	<i>Nemocardium samarangae</i>	Misaki, Kanagawa, Central Japan	
	<i>Tridacna crocea</i>	Honda Bay, Palawan, southwest Philippines	
Mactridae	<i>Mactra chinensis</i>	Wakkanai, Hokkaido, northern Japan	
	<i>M. veneriformis</i>	Misaki, Kanagawa, Central Japan	
	<i>Pseudocardium sachalinense</i>	Sarufutsu, Hokkaido, northern Japan	
Tellinidae	<i>Tellina venulosa</i>	Sarufutsu, Hokkaido, northern Japan	
Psammobiidae	<i>Solecurtus divaricatus</i>	Morozaki, Aichi, Central Japan	
Glossidae	<i>Meiocardia tetragona</i>	Misaki, Kanagawa, Central Japan	
Corbiculidae	<i>Corbicula sandai</i>	Lake Biwa, Shiga, Central Japan	
Veneridae	<i>Venus foveolata</i>	Shima, Mie, Central Japan	
	<i>Periglypta puerpera</i>	Honda Bay, Palawan, southwest Philippines	
	<i>Circe scripta</i>	Sagami Bay, Kanagawa, Central Japan	
	<i>Gafrarium tumidum</i>	Iriomote Is., Okinawa, southwest Japan	
	<i>Callanaitis disjecta</i>	Australia	
	<i>Anomalocardia brasiliiana</i>	Brazil	
	<i>Placamen tiara</i>	Shima, Mie, Central Japan	
	<i>Mercenaria stimponi</i>	Wakkanai, Hokkaido, northern Japan	
	<i>M. cyprinoides</i>	Danvers, Massachusetts, USA	
	<i>M. mercenaria</i>	Danvers, Massachusetts, USA	
	<i>Protothaca euglypta</i>	Misaki, Kanagawa, Central Japan	
	<i>P. jodoensis</i>	Misaki, Kanagawa, Central Japan	
	<i>Timoclea micra</i>	Shikanoshima, Fukuoka, western Japan	
	<i>Meretrix petechialis</i>	Morozaki, Aichi, Central Japan	
	<i>Callista brevisiphonata</i>	Sarufutsu, Hokkaido, northern Japan	
	<i>Saxidomus purpuratus</i>	Morozaki, Aichi, Central Japan	
	<i>Ruditapes philippinarum</i>	Misaki, Kanagawa, Central Japan	
	<i>Kateleyisia japonica</i>	Iriomote Is., Okinawa, southwest Japan	
	<i>Paphia schnelliana</i>	Sagami Bay, Kanagawa, Central Japan	
	<i>P. anabilis</i>	Sagami Bay, Kanagawa, Central Japan	
	<i>P. euglypta</i>	Sagami Bay, Kanagawa, Central Japan	
	<i>Phacosoma japonicum</i>	Misaki, Kanagawa, Central Japan	
	<i>Clementia vatheleti</i>	Shima, Mie, Central Japan	
	<i>Cyclina sinensis</i>	Ariake, Saga, western Japan	
	Corbulidae	<i>Solidicorbula erythron</i>	Morozaki, Aichi, Central Japan
	Hiatellidae	<i>Hiatella orientalis</i>	Misaki, Kanagawa, Central Japan
	Pholadidae	<i>Zirfaea crispata</i>	California, USA
Cuspidaridae	<i>Cuspidaria hindsiana</i>	Misaki, Kanagawa, Central Japan	
	<i>C. nobilis</i>	Misaki, Kanagawa, Central Japan	

gypsum and polished with graded powder. The polished plane was etched with 5% acetic acid for several minutes, washed, and dried in air. For optical microscopy an acetate peel was prepared for each specimen by pressing a sheet of triacetylcellulose film (25 μm in thickness) onto the etched surface flooded with acetone (Kennish *et al.*, 1980). Thin sections were made for fossil specimens. The acetate peels and the thin sections were observed with an Olympus AHBT optical microscope. Polished and etched surfaces of selected specimens were coated with platinum vanadium using an Eiko IB-5 ion coater and examined with a Hitachi S-2400 scanning electron microscope operated at 15 kV.

For the computer simulation of the shell section, a program written in N-88 BASIC was carried out with a personal computer (NEC PC-9821Xp) interfaced with a CRT (SANYO CMT-B15M6) and an ink-jet printer (Canon BJC-600J).

Geometric pattern of shell section and remarks on sculpture formation

Internal microgrowth increments

In many species, internal microgrowth increments consist of regularly arranged straight lines with elliptic or sigmoid curves which are mutually parallel in sections (Figures 1-1, 1-2). They maintain a similar basic morphology during growth which is independent of the sculptural pattern. This type of microgrowth increments is tentatively called **the regular type**. In *Anodonta woodiana*, *Cristaria plicata*, *Chlamys swifti*, *Clementia vatheleti*, *Cuspidaria nobilis*, *Cuspidaria hindsiana*, *Inoceramus hobetsensis* (Figure 1-3), and *Inoceramus uwajimensis*, microgrowth increments prominently undulate along the plicated sculpture. Consequently, the shells of these species consist of prisms or lamellae which are not parallel to one another (Figure 1-4). This type of increment is here called **the undulated type**.

In *Inversidens reiniana* and *Pseudocardium sachalinense*, morphology of microgrowth increments is occasionally disturbed at a localized part in the outermost portion (Figure 1-5). Weak undulation or disturbance of microgrowth increments was occasionally found in *Mytilus galloprovincialis* (Figure 1-6), *Mytilus californianus* and *Modiolus modiolus*. In *Tridonta alaskensis* (Figure 1-7), *Lamprotula rochechoarti* and *Solecurtus divaricatus*, microgrowth increments in the outermost shell layer slightly change their shape in the distal part during growth. They are sigmoid-shaped near the ridge of the sculpture, but such a feature disappears in the groove. The morphology of increments of these species mentioned

above seems to be an intermediate between the regular and undulated types, but the undulation of the increments is generally weak, and this type essentially belongs to the regular type in substance.

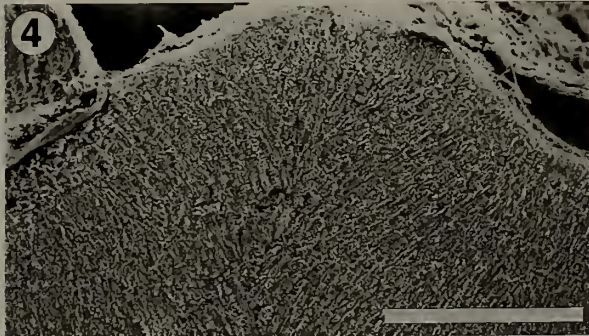
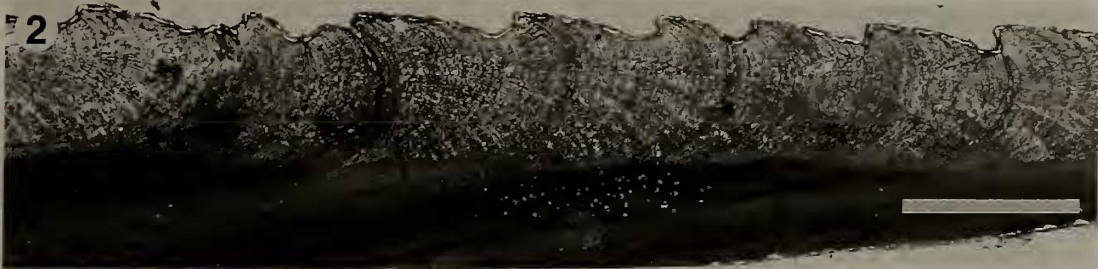
If mantle deformation is restricted to lateral extension and shrinkage, and if the mantle does not heave or bend, internal microgrowth increments, which are trails of mantle movement, maintain their direction mutually parallel to one another. But if the mantle edge bulges or bends, the stacking pattern of microgrowth increments is disturbed and they change their direction in limited parts of the shell. The basic morphology of the regular-type microgrowth increments is maintained during growth, and is independent of sculptural pattern. From the above arguments, it is expected that in the species with the regular-type increments, the mantle deformation is restricted to lateral extension and shrinkage along the inner surface of the shell in substance. Conversely, in the case of the undulated type of increments, the mantle edge is considered to heave or bend.

Remarks on sculpture with undulated type of increments

In many bivalve species, wave phases of the ridges and furrows on a valve usually correspond to those of the other valve. However in *Anodonta woodiana*, *Cristaria plicata*, which have the undulated type of increments, folds alternately occur on the left and right valves, so that the ridges on one valve correspond to furrows on the opposite valve (see also Savazzi and Peiyi, 1992). In *Anodonta woodiana* and *Cristaria plicata*, ribs are often oblique to the commarginal growth lines on the external shell surface (Figure 2-4), namely the sculpture is not perfectly commarginal. In this case, a bivalve cannot close its valves tightly without phase difference of the plicae between both valves. The plicated fold of *Inoceramus hobetsensis* sometimes runs obliquely across the commarginal growth lines. In *Inoceramus hobetsensis*, it is presumed that the folds on one valve correspond to furrows on the opposite valve, even though no specimen of this species, which has slightly oblique ribs, with the valves conjoined was found.

It is evident that plicated folds with the undulated type of increments reflect the topography of the wavy mantle surface which acts as a template for shell formation. Slight obliquity of the sculpture in *Anodonta woodiana* (Figure 2-4), *Cristaria plicata* and *Inoceramus hobetsensis* suggests that the phase of topographic condition of the mantle waving shifts along the mantle margin during growth. In these three species, plicae are built alternatively on both valves. These

Figure 1. Photographs of the lateral view of the bivalve shell in radial sections. The outer surface of the shell is upward and the ventral side to the right. Arrows indicate the myostracum. 1. Optical micrograph of peeled section of *Paphia schnelli* from Sagami Bay, Kanagawa, Central Japan (UMUT RM 27340). Scale bar: 500 μm . 2. Optical micrograph of peeled section of *Phacosoma japonicum* from Misaki, Kanagawa, Central Japan (UMUT RM 27341). Scale bar: 1 mm. 3. Broken section of a giant shell of *Inoceramus hobetsensis* from Turonian (Cretaceous) bed in Obira, Hokkaido, northern Japan (UMUT MM 27342). Scale bar: 3 cm. 4. Scanning electron micrograph of *Cuspidaria hindsiana* from Misaki, Kanagawa, Central Japan (UMUT RM 27343). Scale bar: 200 μm . 5. Optical micrograph of peeled section of *Pseudocardium sachalinense* from Sarufutsu, Hokkaido, northern Japan (UMUT RM 27344). Scale bar: 1 mm. 6. Optical micrograph of peeled section of *Mytilus galloprovincialis* from Misaki, Kanagawa, Central Japan (UMUT RM 27345). Scale bar: 1 mm. 7. Optical micrograph of peeled section of *Tridonta alaskensis* from Etorofu Is., Hokkaido, northern Japan (UMUT RM 27346). Scale bar: 1 mm.



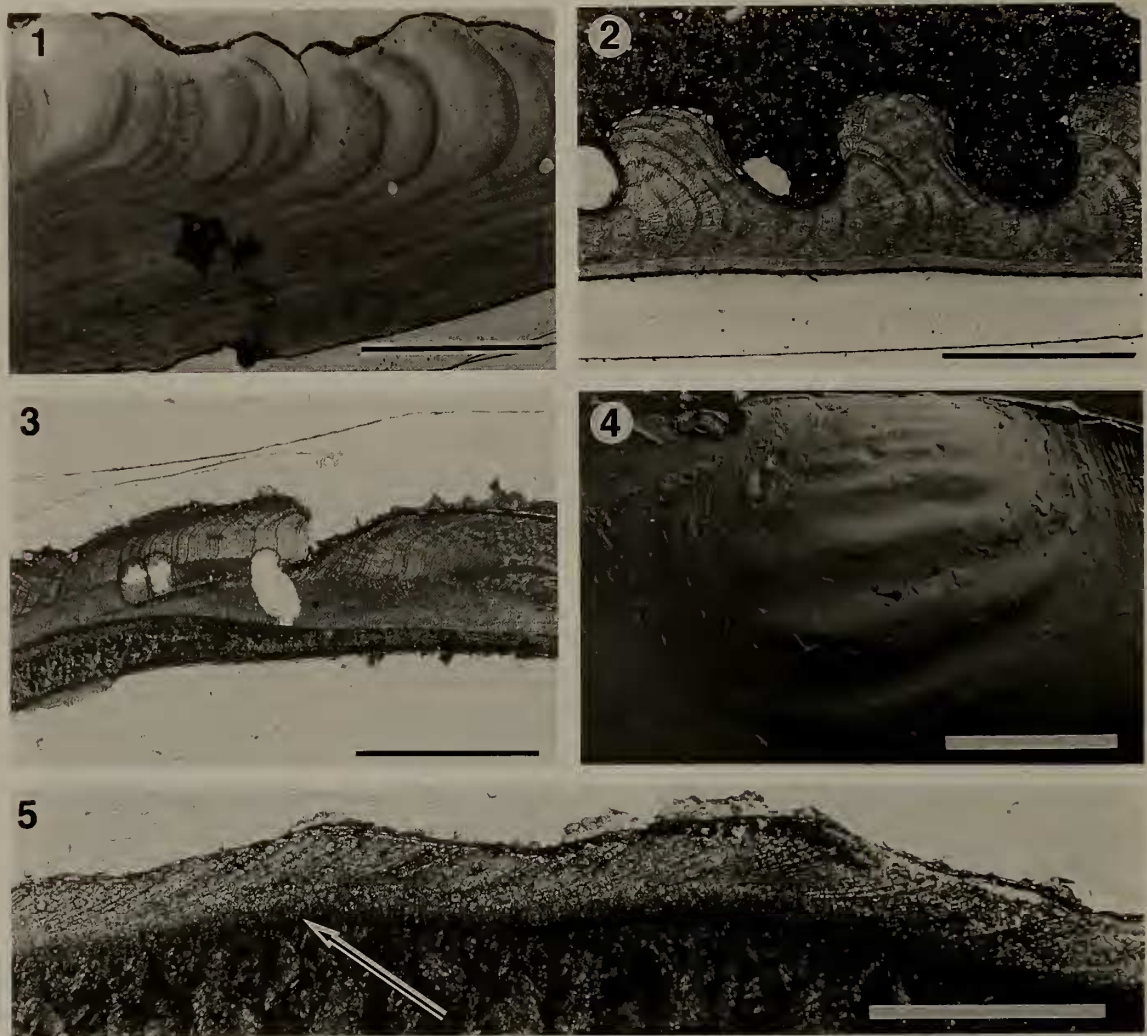


Figure 2. 1-3, 5. Optical micrographs of radial peeled sections. The outer surface of the shell is upward and the ventral side to the right. Arrows indicate the myostracum. 1. *Callista brevisiphonata* from Sarufutsu, Hokkaido, northern Japan (UMUT RM 27347). Scale bar: 2 mm. 2. *Paphia amabilis* from Sagami Bay, Kanagawa, Central Japan (UMUT RM 27348). Scale bar: 1 mm. 3. *Megacardita ferruginosa* from Misaki, Kanagawa, Central Japan (UMUT RM 27349). Scale bar: 2 mm. 4. Lateral view of the valve of *Anodonta woodiana* from Lake Biwa, Shiga, Central Japan (UMUT RM 27350). Scale bar: 2 cm. 5. *Meiocardia tetragona* from Misaki, Kanagawa, Central Japan (UMUT RM 27351). Scale bar: 1 mm.

facts indicate that mantles on the left and right sides bend in the same direction and that commarginal waves are formed on the mantles, namely, commarginal shell sculpture appears to originate from mantle bending on the left and right sides and the subsequent shell folding. On the other hand, in *Chlamys swifti*, *Clementia vatheleti* and *Cuspidaria* spp., each commarginal ridge on a valve matches that on the opposite valve, showing that bulging of the mantles on both sides or swelling of the visceral mass is the likely factor. In these four species, sculpture formation is explained by the bulging or rising of mantle edges on both sides.

Remarks on sculpture with regular type of increments

The accretionary pattern of regular type internal microgrowth increments is not always conformable to that of the sculpturing phase on the shell. For example, in *Tridonta alaskensis*, *Tridacna crocea*, *Meiocardia tetragona*, *Corbicula sandai*, *Circe scripta*, *Gafrarium tumidum*, *Anomalocardia brasiliensis*, *Katelsysia japonica*, *Paphia schnelliensis* (Figure 1-1), *Paphia amabilis* (Figure 2-2), *Phacosoma japonicum* (Figure 1-2), and other many species, the increments are generally irregularly spaced and their periodic patterns appear to be independent of the sculptural pattern. The accretionary patterns of internal microgrowth increments in such species are considered to be affected by environmental factors

(Pannella and MacClintock, 1968 ; Lutz and Rhoads, 1977 ; Jones, 1985). In all probability, the effect of environmental fluctuations on shell precipitation seems to be not strong enough to build the sculpture in such species. If so, what growth components form the sculpture in such species ?

On the contrary, in *Callista brevisiphonata* (Figure 2-1), *Pseudocardium sachalinense* and *Mytilus grayanus*, the regular-type increments tend to be densely arranged on the ventral side of the slope in going from the ridge to the furrow of the costae. An irregular and incidental furrow is occasionally accompanied by a condensed band of regular-type increments in *Arca navicularis*, *Glycymeris yessoensis*, *Megacardita ferruginosa* (Figure 2-3), *Solecrtus divaricatus*, *Timoclea micra* and *Protothaca euglypta*. Does fluctuation of the precipitation rate of calcium carbonate cause the sculpture formation in such cases ?

In many species with the regular type of increments, the myostracum is generally smooth, independent of sculpturing

(Figures 1-1, 1-7, 2-2). However, a weak undulation of the myostracum is occasionally found in *Barbatia amygdarumtorum*, *Megacardita ferruginosa*, *Meiocardia tetragona* (Figure 2-5), *Mytilus californianus* and *Modiolus modiolus*. What determines the geometry of myostracum through the sculpture construction ?

Theoretical morphology of shell section with regular type increments

Modeling of growth kinematics

In order to recognize clearly growth components controlling the sculpture formation, and to estimate theoretical spectrum of geometric pattern of the shell section, the microscopic shell growth with the regular type of increments is modeled theoretically.

Let us consider the process of shell growth in Figure 3. The shell growth in radial sections during a short period of

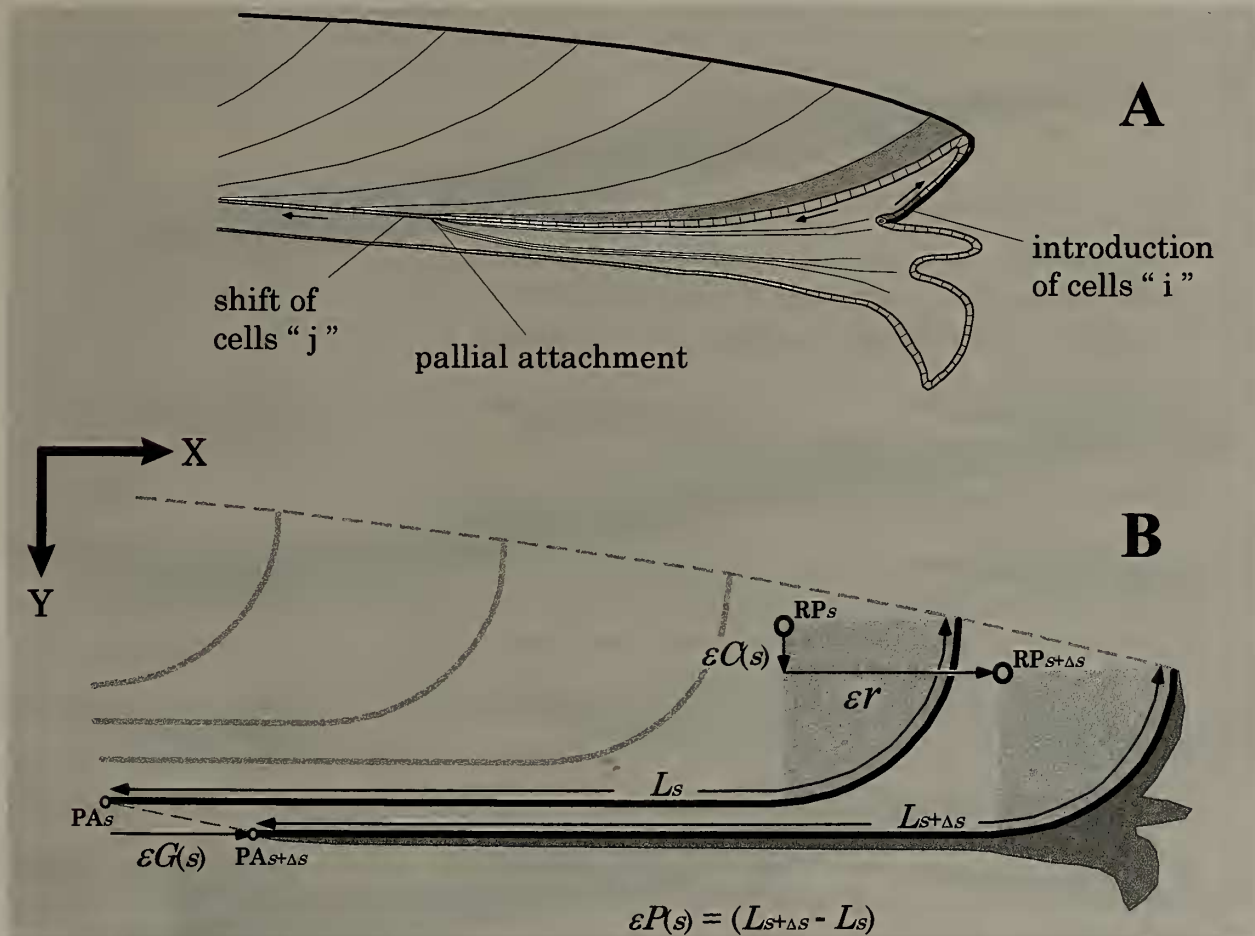


Figure 3. Schematic diagrams of the shell edge of a bivalve showing the model of growth process during a short period of time. **A.** In a growth stage, cells "i" arise from the mantle edge and the cells "j" at the pallial attachment shift by formation of cells "i", and the secretory product of the cells "j" alters from myostracum to inner shell layer. **B.** During a growth stage Δs , the reference point RP_s shifts by ϵr where r is equal to the radius of the circular arc of the increment curve, the pallial attachment point translates from PA_s to $PA_{s+\Delta s}$ and the distal part of the mantle changes its length from L_s to $L_{s+\Delta s}$.

time is exhibited by kinematics of an internal microgrowth increment. Growth components are expressed as functions of growth stage s , rather than as functions of time, since the time scale of the growth process is hardly detected in many cases. The position of a microgrowth increment at a growth stage s is shown by the reference point $RP_s(x_{rs}, y_{rs})$. On the ventral side to the reference point the morphology of a microgrowth increment is represented by a circular arc whose radius is expressed as r , while on the dorsal side it is exhibited by a straight line (Figure 3B). The translation of the internal microgrowth increment is described by the three growth parameters $C(s)$, $G(s)$ and $P(s)$, defined below.

Over a short period of growth step Δs , the mantle secretes calcium carbonate on the inner surface of the shell giving rise to the stippled area in Figure 3A, an area which is analogous to Lison's (1949) matrix. If the reference point

moves to the right by εr parallel to the X axis during the growth step, the reference point shifts below by $\varepsilon C(s)$ parallel to the Y axis, where ε is an arbitrary constant reflecting the magnitude of growth step. The value of $\varepsilon C(s)$ represents the amount of shell precipitation on the inner surface of the outer shell layer. Meantime the pallial attachment point $PA_s(xa_s, ya_s)$ linearly shifts to $PA_{s+\Delta s}(xa_{s+\Delta s}, ya_{s+\Delta s})$ (Figure 3B). Then we express the displacement of the X coordinate of PA_s over the growth step by $\varepsilon G(s)$ which exhibits progression of the pallial attachment. While calcium carbonate is secreted, the mantle proliferates and changes its length by division of epithelial cells. The outer epithelial cells of the mantle mainly arise from the periostracal groove, and successive introduction of cells pushes the earlier produced cells out into the more proximal part of the mantle (Figure 3A). Then the function of the cells change from perios-

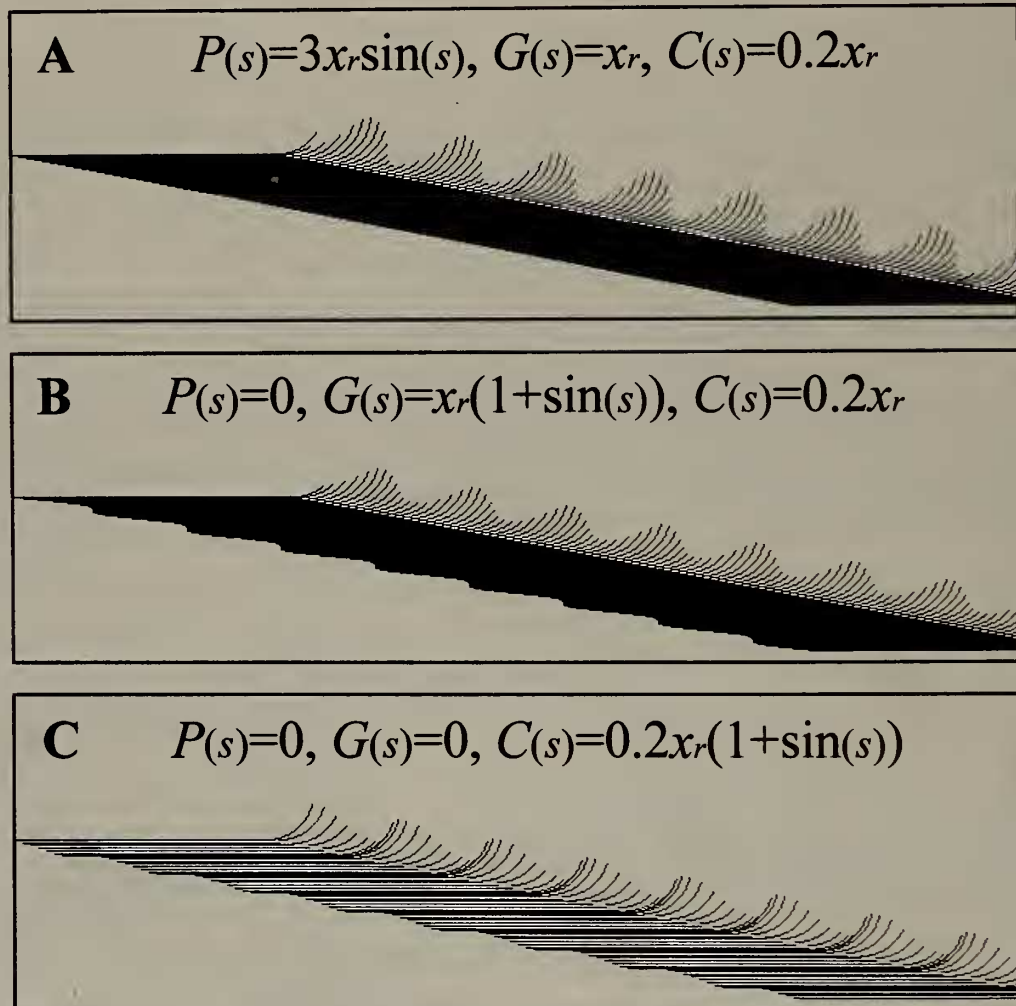


Figure 4. Computer simulations of the bivalve shell in radial sections, showing geometric patterns of microgrowth increments and external sculpture. Only the effect of oscillation of one parameter is considered. The value of x_r represents the X coordinate of the reference point. **A.** The effect of mantle extension and shrinkage is simulated. **B.** The effect of oscillation of mantle proliferation rates is simulated. **C.** The effect of fluctuation in shell precipitation rates is simulated.

tracum secretion to shell secretion or connection to the shell (Stasek and McWilliams, 1973). Consequently, for quite a short period of time, the proliferation of the mantle cells can be approximated by the progression of the pallial attachment from PA_s to $PA_{s+\Delta s}$, even though the progression of pallial attachment represents the growth of visceral mass and is indeed slightly slower than the mantle growth rate throughout ontogeny. The mantle as a whole is a kind of hydroskeleton supported by blood pressure (Morita, 1991) and can be shrunk by the radial pallial muscle. Consequently, if we express the length from PA_s to the mantle edge along the increment by L_s , its value may be changed by mantle extension or shrinkage. Then, the value of $\epsilon P(s)$ is defined by the difference of L_s during the growth step Δs . In general, three growth parameters are defined as follows:

$$C(s) = \frac{y_{rs+\Delta s} - y_{rs}}{\epsilon}, \quad G(s) = \frac{x_{rs+\Delta s} - x_{rs}}{\epsilon},$$

$$P(s) = \frac{L_{s+\Delta s} - L_s}{\epsilon}$$

The sculptural pattern of a bivalve shell in the radial sections is generally more or less periodic and originates by fluctuation of some parameters given by a periodic function. Then, a constant or a periodic function is given for each

parameter. The formulation of the periodic function is considered to be variable depending on the physiological nature of a species and is arbitrarily chosen. In the present simulations, a sine curve function for the periodic oscillation of parameters is chosen. Although three parameters $C(s)$, $G(s)$ and $P(s)$ are incremental components and must increase with size of the whole animal, the zero growth of $P(s)$ is assumed for a limited part of the shell section, namely the mean of $P(s)$ is zero in this model.

Computer simulation of shell section

Firstly, a case was considered in which only one of the three parameters, $C(s)$, $G(s)$ and $P(s)$ oscillates, with the remaining two being fixed. Figure 4 shows computer-produced shell sections for three cases. The trail of the mantle edge during growth becomes wavy in each case, demonstrating that the commarginal sculpture can be produced in any of these conditions. In each case, topography of the shell surface, which varies depending on the given initial microgrowth increment morphology, is not a useful criterion for estimating the origin of the sculpture. But significant characters such as the trail of the pallial attachment, i.e., myostracum, and the interval of microgrowth increments are different among the three cases. When $P(s)$

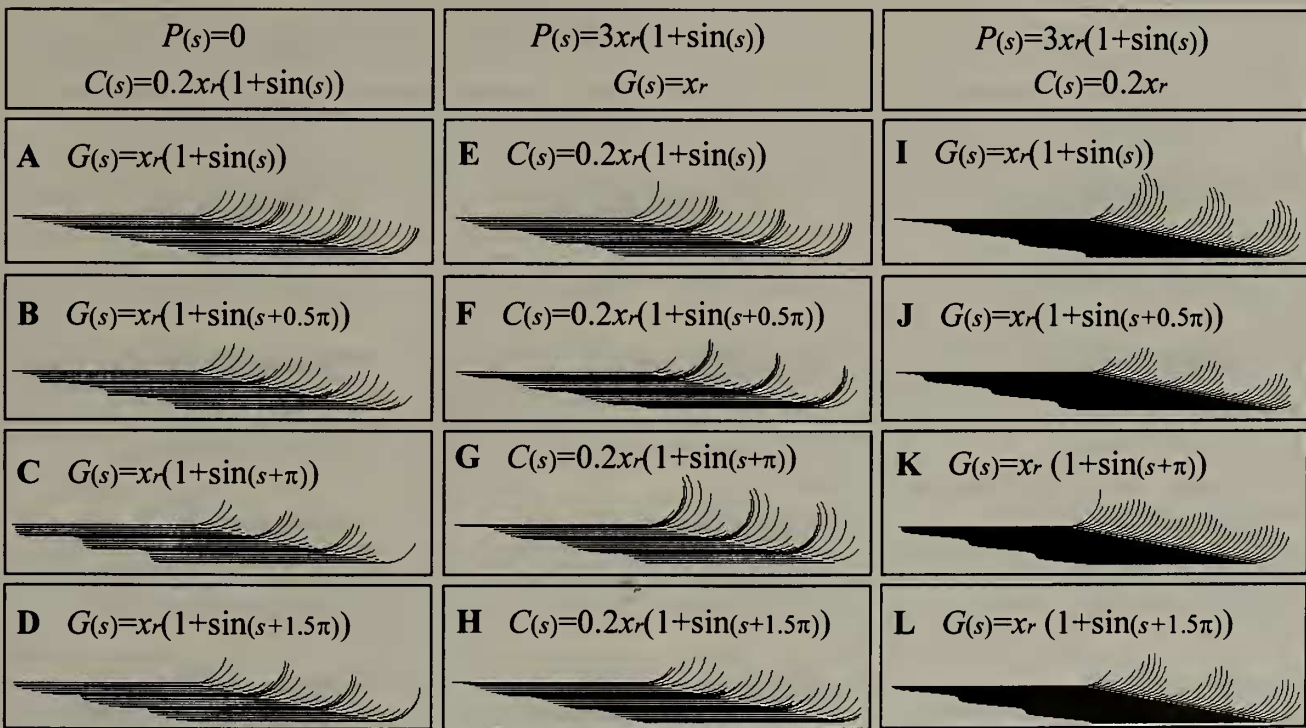


Figure 5. Computer simulations for external shell sculpture and internal microgrowth increments in radial sections as two parameters fluctuate by sine curve functions. This shows the effects of phase difference between two given sine-curve functions for two parameters. The value of x_r represents the X coordinate of the reference point. **A-D.** The progression rates of the pallial attachment and shell precipitation both oscillate, and mantle does not deform. **E-H.** Mantle extends and shrinks, rate of shell precipitation is changed, and the progression rate of the pallial attachment is fixed. **I-L.** Mantle extends and shrinks, the progression rate of the pallial attachment is fluctuated, and the rate of shell precipitation is constant.

oscillates and the other parameters are fixed, the myostracum does not undulate and the interval of increments remains unchanged (Figure 4A). When only $G(s)$ oscillates, the interval of microgrowth increments is also unchanged, but the myostracum undulates (Figure 4B). When only $C(s)$ oscillates, periodically narrowing microgrowth increments are inevitably produced (Figure 4C). In this case, microgrowth increments are densely arranged on the slope of the sculpture from a furrow to a ridge, i.e., on the dorsal side. The myostracum also undulates by $C(s)$ oscillation because the pallial attachment does not translate linearly.

Secondly, let us consider the case when two parameters both oscillate by a sine curve function with a constant wavelength. Figure 5 shows some examples of computer-produced diagrams, illustrating the effects of changes in the phase difference between the two given sine curves for variable parameters. Morphology of the external sculpture is variable depending upon the phase difference. When external sculpture and undulation of myostracum originate by oscillations of $C(s)$ and $G(s)$, microgrowth increments tend to be crowded on the dorsal side of the sculptural slope (Figures 5B-D), while they do not conspicuously develop if the phase of oscillation of $C(s)$ is the same as that of $G(s)$ because effects of fluctuation of $C(s)$ and $G(s)$ are compensated by each other (Figure 5A). When $C(s)$ and $P(s)$ both

oscillate and $G(s)$ is fixed, the myostracum inevitably undulates and the sculpture is constructed (Figures 5E-H). Under this condition, microgrowth increments also tend to be crowded on the dorsal side of the sculptural slope (Figures 5F-H), but the sculpture becomes weak when the phase of $P(s)$ is the same as that of $C(s)$ because of compensating relationships between them (Figure 5E). When both $G(s)$ and $P(s)$ oscillate and contribute sculpture formation, the interval of microgrowth increments has a fixed value during growth and the myostracum always becomes wavy (Figures 5I-L). In this case, if the phase of $G(s)$ lags 180° behind that of $P(s)$, the sculpture becomes relatively weak because of the compensating relationship between them (Figure 5K).

Thirdly, let us consider the case in which all the three parameters oscillate by a sine curve with the same wavelength. Figure 6 shows computer-produced figures illustrating the effects of phase lag of $P(s)$, $G(s)$ or $C(s)$ behind the remaining two parameters whose fluctuation effects are compensated by each other. When $C(s)$ and $G(s)$ oscillate without a phase difference, the myostracum does not undulate because of compensating relationships between them (Figures 6A-E, J), the case in which sculpture originates by $P(s)$ oscillation. In other cases, the myostracum becomes wavy by fluctuation effects of $C(s)$ and $G(s)$. When the phase of $P(s)$ is the same as that of $C(s)$, effects of fluctuation

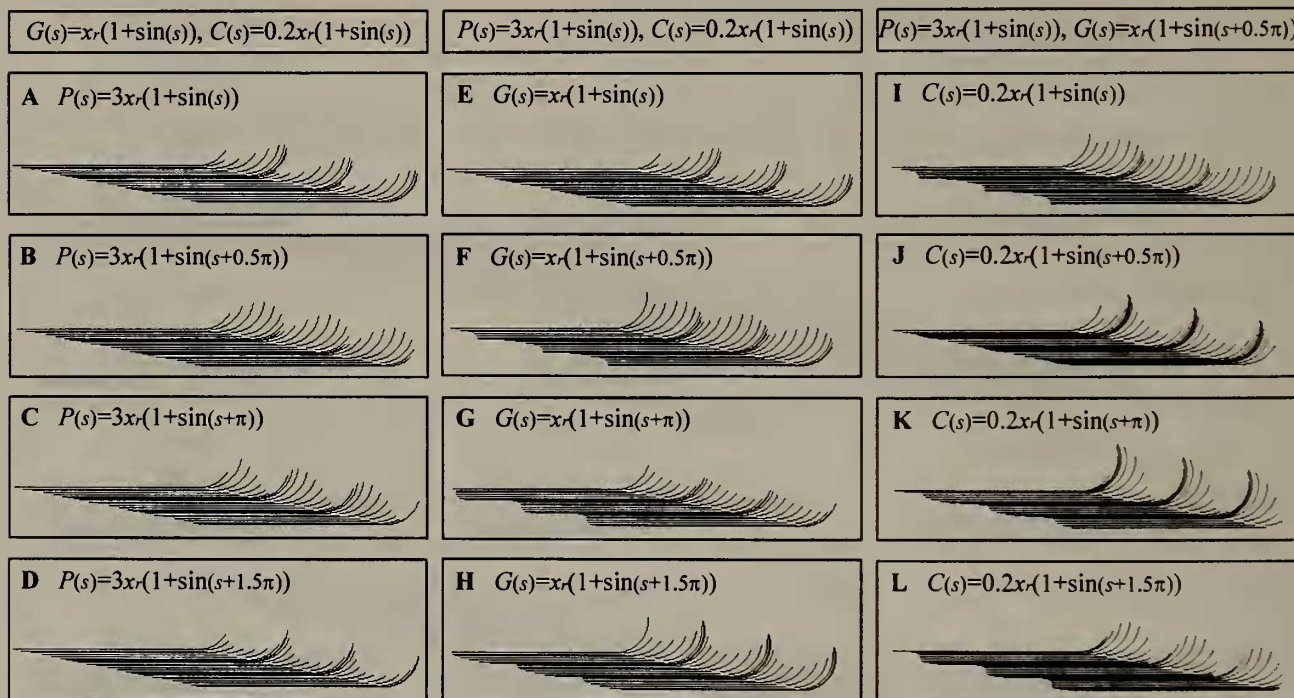


Figure 5. Computer simulations for shell sculpture and increments in the sections showing the effects of phase difference among three oscillating parameters by sine curve functions. The value of x_r represents the X coordinate of the reference point. **A-D.** The effect of $P(s)$ oscillation is taken into consideration in the case of Figure 5A. Phase of $P(s)$ fluctuation is deferred from the other two parameters. **E-H.** Fluctuation effect of $G(s)$ is taken into consideration in the case of Figure 5E. Phase of $G(s)$ oscillation is deferred from the other two. **I-L.** The effect of $C(s)$ oscillation is taken into consideration in the case of Figure 5K. Phase of $C(s)$ fluctuation is different from the others.



profile of myostracum	straight	undulated
pattern of increments		
condense on dorsal slope	A $P(s), C(s)$	D $C(s), G(s)$
condense on ventral slope	B $P(s), G(s)$	E $G(s)$
independent of sculpturing	C $P(s)$	F $P(s), G(s)$

Figure 7. Summary of computer simulations showing what parameters may be effective in shell sculpturing. If myostracum is not wavy in its profile, fluctuation of $P(s)$ is considered to be a main factor of sculpture construction (A-C), while oscillation of $G(s)$ may be more effective in shell sculpturing when myostracum becomes wavy (D-F).

of these two parameters compensate each other and $G(s)$ oscillation causes sculpture formation (Figures 6A, E-H, I). When $G(s)$ lags 180° in phase behind that of $P(s)$, effects of fluctuation of them also compensate for each other and fluctuation of $C(s)$ is the origin of shell sculpturing (Figures 6B, F, I-L). However, in the case of Figure 6C or Figure 6K, the sculpture is regarded to originate by the interaction of $P(s)$ and $C(s)$ oscillations since fluctuation effect of $G(s)$ compensates for those of remaining two parameters. For the same reason, in the case of Figure 6A or Figure 6E, the sculpture is regarded to be produced by the interaction of $P(s)$ and $G(s)$ oscillations. Microgrowth increments generally condense on the dorsal slope of the sculpture when phase of $P(s)$ lags 180° behind that of $G(s)$ (Figures 6I-L). In other cases, the relationship between the phase of commarginal sculpture and the pattern of microgrowth increments becomes variable and depends upon the phase lag of $P(s)$ or $G(s)$ behind the remaining two parameters (Figures 6A-D, E-H).

To sum up the results of the computer simulations, the theoretical spectrum of geometric pattern of the shell section is obtained, and we can identify effective factors on sculpturing for each case when the growth pattern of the microgr-

owth increment and the morphology of myostracum are given (Figure 7). When the myostracum does not undulate, oscillation of $P(s)$ caused by mantle extension and shrinkage mainly contributes to sculpture construction (Figures 7A-C). If the myostracum is wavy, oscillation of $G(s)$ mainly causes the sculpture (Figures 7D-F).

Origin of commarginal shell sculpture with regular type of increments

Although the regular-type increments tend to be densely arranged on the ventral side of the slope or at the furrow of the sculpture in *Arca navicularis*, *Glycymeris yessoensis*, *Callista brevisiphonata*, *Paphia schnelliana*, *Megacardia ferruginosa* (Figure 2-3), *Solecortus divaricatus*, *Timoclea micra* and *Protothaca euglypta*, the pattern of microgrowth increments such as shown in Figure 7 was not found in the specimens examined. The results of computer simulations show that the fluctuation of precipitation rates of the shell $C(s)$ does not influence the sculpture formation. In addition, in many species with the regular-type increments, the myostracum does not prominently undulate. In this case we can identify the factor of sculpturing as the mantle extension-shrinkage and/or changes in progression rates of the

pallial attachment (Figures 7B, C). The undulating myostracum, whose wavy phase corresponds to that of the sculpture, is only found in *Barbatia amygdarumtortum*, *Meiocardia tetragona* and *Mytilus californianus*. However, such an undulation is generally weak and is not enough to construct a prominent sculpture by itself. In this case, mantle extension-shrinkage movement surely contributes to the sculpture formation (Figure 7C).

In *Isognomon perna*, *Lamprotula* sp., *Tridonta alaskensis*, *Codakia tigerina*, *Mercenaria cyprinoides*, *Meretrix petechialis* and *Katylsia japonica*, all of which possess two sublayers of different shell microstructure or coloration in the outer shell layer, the boundary between the outermost and middle sublayers often oscillates (Figures 1-2, 1-7). This fact suggests that the relative position of epithelia secreting each sublayer is almost fixed on the mantle during a short period of time, and that the mantle extension-shrinkage movement causes swinging of the boundary between the two clusters of epithelial cells on the mantle edge.

Concluding remarks

From the comparison of the results of computer simulation with microscopic observation of actual specimens, it was made clear that in species with regular-type increments, the commarginal shell sculpture is mainly constructed by mantle extension and shrinkage by blood pressure and pallial muscle contraction, while fluctuations of shell precipitation rates do not affect sculpture formation. On the other hand, in species with undulated-type increments, the commarginal shell sculpture is produced by mantle heaving or bending, the pattern of which cannot be represented by computer simulation in this study. In any case, it is concluded that periodic state change of the mantle-shell relationship associated with sculpture formation originates in elastic deformation of the distal part of the mantle. The above discussion deals with the two-dimensional pattern of the microscopic feature in the radial shell section, but is essentially valid in three-dimensional morphology as far as the commarginal sculpturing is concerned. Since internal growth pattern of the shell is often preserved in fossils, constructional morphology of shell section could reveal the process of the microscopic-level growth and mantle movements of fossil bivalves.

The morphology of external shell sculpture is quite variable in actual specimens. They are strongly influenced by the shape and direction of each microgrowth increment which is constrained by the crystal growth in the shell (Ubukata 1994, 1997). For example, in *Codakia tigerina*, *Gafrarium tumidum*, *Anomalocardia brasiliensis*, *Mercenaria stimpsoni*, *Periglypta puerpera*, *Fragum unedo*, and *Phacosoma japonicum* (Figure 1-2), ridges are prominently tilted and asymmetrical like saw teeth, and prisms or lamellae radiate from the central longitudinal axis in the outer shell layer (Carter and Clark, 1985; Carter et al., 1991); accordingly, a saw like thread is more easily formed in such species by mantle extension and shrinkage. On the other hand, in *Inoceramus uwajimensis*, *Pinctada margaritifera*, *Isognomon legmen*, *Malleus regula*, *Atrina kinoshitai*, *Anodonta woodiana*, and *Modiolus*

modiolus, for instance, each microstructural unit of the outer shell layer grows from the periostracum to the mantle. In this case, it is easy to program imbricated lamellae by rhythmic mantle extension-shrinkage or plicated folds by periodic mantle bulging or bending (Figure 1-3). The saw like thread sculpture may be suitable for burrowing (Seilacher, 1974), while the imbricated lamellae are considered to resist burial movement but may serve a stabilizing function for shallow burrowers (Stanley, 1970). Plicated folds seem to provide mechanical strength for thin shells (Stanley, 1970). If a close relationship between the commarginal sculpture and habitat exist, functional morphology and diversity of the commarginal sculpture can be attained with variation of mantle behavior in bivalves.

Acknowledgments

I thank Kazushige Tanabe (University of Tokyo), Takashi Okamoto (Ehime University), Rihito Morita (Natural History Museum and Institute, Chiba), Tatsuo Oji, Kazuyoshi Endo (University of Tokyo), Tomoki Kase (National Science Museum, Tokyo) and the anonymous referee of *Paleontological Research* for critical reviews of the manuscript and for valuable comments. Thanks to James J. Cabrera (National Museum, Manila) and Research Institute of Tropical Agriculture, University of the Ryukyus for their help in collecting sample during field work. Shinji Isaji (Natural History Museum and Institute, Chiba), Takenori Sasaki (University of Tokyo) and Saori Nakai provided me some samples. This study has been partly subsidized by the Grants-in-Aid of Ministry of Education, Science and Culture, Japan for JSPS Research Fellow (No. 3695 in 1995) and for International Scientific Research Program (No. 04041085 in 1993). This research was also partly supported by the Grants-in-Aid of Fujiwara Natural History Foundation in 1993.

References

- Ackerly, S.C., 1992: The origin and geometry of radial ribbing patterns in articulate brachiopods. *Lethaia*, vol. 25, p. 243-247.
- Carter, R.M., 1967: On Lison's model of bivalve shell form, and its biological interpretation. *Proceedings of Malacological Society of London*, vol. 37, p. 265-278.
- Carter, J.G. and Clark, G.R. II, 1985: Classification and phylogenetic significance of molluscan shell microstructure. In Broadhead, T.W. ed., *Mollusks: Notes for a Short Course*, p. 15-17. Department of Geological Science, Studies in Geology, B. University of Tennessee, Knoxville.
- Carter, J.G., Bandel, K., de Buffrenil, V., Carlson, S., Castanet, J., Dalingwater, J., Francillon-Vieillot, H., Geraudie, J., Meunier, F.J., Mutvei, H., de Ricoles, A., Sire, J.Y., Smith, A., Wendt, J., Williams, A. and Zylberberg, L., 1991: Glossary of skeletal biomineralization. In Carter, J.G. ed., *Skeletal Biomineralization: Pattern, Process and Evolutionary Trends*, vol. 1, p. 337-399. Van Nostrand, New York.
- Checa, A., 1994: A model for the morphogenesis of ribs in ammonites inferred from associated microsculptures.

- Palaeontology*, vol. 37, p. 863-888.
- Cox, L.R., 1969: General features of Bivalvia. In, Moore, R.C. ed., *Treatise on Invertebrate Paleontology, Mollusca 6, Bivalvia*, p. 2-129. Geological Society of America and University of Kansas Press, Lawrence.
- Gunji, Y., 1990: Pigment color patterns of molluscs as an autonomous process generated by asynchronous automata. *Biosystems*, vol. 23, p. 317-334.
- Hayami, I. and Okamoto, T., 1986: Geometric regularity of some oblique sculptures in pectinid and other bivalves: recognition by computer simulations. *Paleobiology*, vol. 12, p. 433-449.
- Jones, D.S., 1985: Growth increments and geochemical variations in the molluscan shells. In, Broadhead, T.W. ed., *Mollusks: Notes for a Short Course*, p. 72-87. Department of Geological Science, Studies in Geology, B. University of Tennessee, Knoxville
- Jones, D.S., Thompson, I. and Ambrose, W., 1978: Age and growth rate determinations for the Atlantic surf clam *Spisula solidissima* (Bivalvia: Mactracea), based on internal growth lines in shell cross-sections. *Marine Biology*, vol. 47, p. 63-70.
- Kennish, M.J., Lutz, R.A. and Rhoads, D.C., 1980: Preparation of acetate peels and fractured sections for observation of growth patterns within the bivalve shell. In, Rhoads, D.C. and Lutz, R.A. eds., *Skeletal Growth of Aquatic Organisms*, p. 597-601. Plenum Publishing Corporation, New York.
- Lindsay, D.T., 1982a: Simulating molluscan shell pigment lines and states: implications for pattern diversity. *The Veliger*, vol. 24, p. 297-299.
- Lindsay, D.T., 1982b: A new programmatic basis for shell pigment patterns in the bivalve mollusc *Lioconcha castrensis* (L.). *Differentiation*, vol. 21, p. 32-36.
- Lison, L., 1949: Recherches sur la forme et la mécanique de développement des coquilles des lamellibranches. *Mémoires de l'Institut Royal des Sciences Naturelles de la Belgique, Série 2*, vol. 34, p. 1-87.
- Lutz, R.A. and Rhoads, D.C., 1977: Anaerobiosis and a theory of growth line formation. *Science*, vol. 198, p. 1222-1227.
- Meinhardt, H., 1984: Models for positional signaling, the threefold subdivision of segments and the pigmentation pattern of molluscs. *Journal of Embryology and Experimental Morphology*, vol. 83, p. 289-311.
- Meinhardt, H. and Klingler, M., 1987: A model for pattern formation on the shell of molluscs. *Journal of Theoretical Biology*, vol. 126, p. 63-89.
- Morita, R., 1991: Finite element analysis of a double membrane tube (DMS-tube) and its implication for gastropod shell morphology. *Journal of Morphology*, vol. 207, p. 81-92.
- Pannella, G. and MacClintock, C., 1968: Biological and environmental rhythms reflected in molluscan shell growth. *Journal of Paleontology, Paleontological Society Memoir*, vol. 2, p. 64-80.
- Rudwick, M.J.S., 1968: Some analytic methods in the study of ontogeny in fossils with accretionary skeletons. *Journal of Paleontology, Paleontological Society Memoir*, vol. 2, p. 35-49.
- Savazzi, E., 1986: Burrowing sculpture and life habits in Paleozoic lingulacean brachiopods. *Paleobiology*, vol. 12, p. 46-63.
- Savazzi, E., 1990: Biological aspects of theoretical shell morphology. *Lethaia*, vol. 23, p. 195-212.
- Savazzi, E., Jefferies, R.P.S. and Signor, P.W. III., 1982: Modification of the paradigm for burrowing ribs in various gastropods, crustaceans and calcichordates. *Neues Jahrbuch für Geologie und Paläontologie, Abhandlungen*, vol. 164, p. 206-217.
- Savazzi, E. and Peiyi, Y., 1992: Some morphological adaptations in freshwater bivalves. *Lethaia*, vol. 25, p. 195-209.
- Seilacher, A., 1972: Divaricate patterns in pelecypod shells. *Lethaia*, vol. 5, p. 325-343.
- Seilacher, A., 1974: Fabricational noise in adaptive morphology. *Systematic Zoology*, vol. 22, p. 451-465.
- Seilacher, A., 1985: Bivalve morphology and function. In, Broadhead, T.W. ed., *Mollusks: Notes for a Short Course*, p. 88-101. Department of Geological Science, Studies in Geology, B. University of Tennessee, Knoxville.
- Seilacher, A. and Gunji, P.Y., 1993: Morphogenetic count-downs in heteromorph shells. *Neues Jahrbuch für Geologie und Paläontologie, Abhandlungen*, vol. 190, p. 237-265.
- Signor, P.W. III., 1982: Constructional morphology of gastropod ratchet sculpture. *Neues Jahrbuch für Geologie und Paläontologie, Abhandlungen*, vol. 163, p. 349-368.
- Stanley, S.M., 1969: Bivalve mollusk burrowing aided by discordant shell ornamentation. *Science*, vol. 166, p. 634-635.
- Stanley, S.M., 1970: Relation of shell form to life habit in the Bivalvia (Mollusca). *Geological Society of America, Memoir*, vol. 125, p. 1-296.
- Stasek, C.R. and McWilliams, W.R., 1973: The comparative morphology and evolution of the molluscan mantle edge. *The Veliger*, vol. 16, p. 1-19.
- Tanabe, K., 1988: Age and growth rate determination of an intertidal bivalve, *Phacosoma japonicum*, using internal shell increments. *Lethaia*, vol. 21, p. 231-241.
- Tanabe, K. and Oba, T., 1988: Latitudinal variations in shell growth patterns of *Phacosoma japonicum* (Bivalvia: Veneridae) from the Japanese coast. *Marine Ecology, Progress Series*, vol. 47, p. 75-82.
- Ubukata, T., 1994: Architectural constraints on the morphogenesis of prismatic structure in Bivalvia. *Palaeontology*, vol. 37, p. 241-261.
- Ubukata, T., 1997: Microscopic growth of bivalve shells and its computer simulation. *The Veliger*, vol. 40, p. 178-190.
- Waddington, C.H. and Cowe, R.J., 1969: Computer simulation of a molluscan pigmentation pattern. *Journal of Theoretical Biology*, vol. 25, p. 219-225.
- Wrigley, A., 1948: The color patterns and sculpture of molluscan shells. *Proceedings of the Malacological Society of London*, vol. 27, p. 206-217.